2017 IEEE Conference on Control Technology and Applications (CCTA)
August 27-30, 2017. Kohala Coast, Hawai'i, USA

Convex Optimization-Based Control of Sustainable Communities with On-Site Photovoltaic (PV) and Batteries*

Jie Cai[1], Hao Zhang[1], Donghun Kim[1], James E. Braun[1] and Jianghai Hu[2]

***Abstract*— This paper presents a convex optimization-based control method for sustainable communities with multiple buildings served by a central cooling plant and with on-site solar generation and batteries. A model predictive control (MPC) approach is used to optimally schedule the energy flows among the different energy sources, on-site battery and building end users to achieve the minimum operation cost. A convex formulation is derived for the MPC problem which is then solved with a convex programming package. With the optimal operation strategy, a 9.4% energy cost savings and a 35.6% demand cost savings were achieved compared to a baseline control strategy, for a case study with three buildings and an on-site PV and battery system.**

I. INTRODUCTION

With fast technology advancements and lower manufacturing costs, on-site renewable generation such as photovoltaic (PV) and wind turbines are becoming more popular for building owners to reduce electricity purchases from the grid and also to lower their electricity costs. On-site renewable generation is often used together with batteries to collect the generated electricity when power demand is moderate and the infrastructure does not allow selling excess power back to the grid. Other advanced energy systems, such as geothermal-assisted heat pumps, district heating and cooling, combined cooling, heating and power, are also attractive to residential and commercial buildings due to their improved energy efficiency. Although the costs of the on-site renewable generation and advanced energy systems have been reduced in recent years, these systems are more widely adopted in a community- or city-level application, and are not commonly used in individual buildings due to less favorable economics. Proper operation of sustainable communities with these features is critical to achieve their full potentials but it is a challenging task due to the large number of optimization variables involved.

Extensive work can be found in the literature that studied the integration of renewable generation in buildings (e.g., [1]-[4]). In [5], a mixed-integer nonlinear programming approach was proposed for optimal scheduling of building energy systems integrated with renewable generation and a thermal storage tank to minimize the operation cost. [6] studied optimal sizing of an on-site PV and energy storage system for a grid-connected residential building through optimizing the load profiles and system operation. In [7], a particle swarm optimization-based decision framework was developed for optimized operation of a building cluster with multiple buildings and on-site PV and energy storage systems. Most of the previous work heavily relied on heuristic optimization or mixed integer programming algorithms which are computationally demanding and cannot guarantee optimal performance.

In this paper, the optimal demand management problem is investigated for sustainable communities with multiple buildings and on-site PV and batteries. A model predictive control (MPC) problem is considered to find the optimal schedules of energy flows among different sources and end users with the minimum operation cost. With certain near-optimal heuristics and specific manipulation, the MPC problem is formulated as a convex optimization problem and is solved with a convex programming solver. To benchmark the cost savings potential associated with the proposed control solution, a baseline strategy is simulated with a conventional night setup/setback indoor temperature control and a rule-based control for charging and discharging the battery.

II. COMPONENT MODELS

Fig. 1 shows the system layout of the sustainable community considered in this study. The community has multiple buildings served by a central cooling plant, which uses an air-cooled chiller in the case study. The chiller provides chilled water at a constant temperature to all buildings. Only the cooling scenario is investigated and a gas furnace is used in each building for space heating. There is an electricity bus to power the central cooling plant and also to satisfy the other electrical uses in the buildings. The power bus can take electricity from PV generation, battery discharge, electricity purchase from the power grid or any combination of the three. The on-site battery can be charged with electricity purchased from the power grid or generated by PV panels. In the following model and optimization formulations, underlined variables are used to highlight the boundary conditions in the optimization problem that are known ahead of time.

A. Building Model

The case study community is assumed to have three commercial buildings. Dynamic building thermal models were developed for three offices at the Center for High Performance Buildings (CHPB) at Purdue University and these three office models are used to represent the three individual buildings in the case study. The models utilize simplified

*Research supported by the National Science Foundation under Grant No. 1329875 and the Center for High Performance Buildings at Purdue University

[1]J. Cai, H. Zhang, D. Kim and J. E. Braun are with School of Mechanical Engineering, West Lafayette, IN 47906 USA (cai40@purdue.edu).

[2]J. Hu are with School of Electrical and Computer Engineering, West Lafayette, IN 47906 USA.

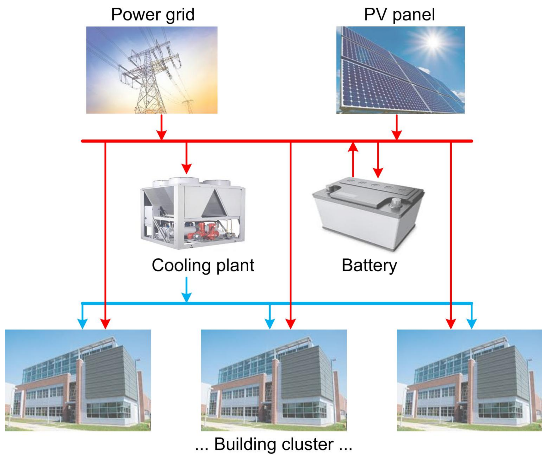

Fig. 1. A sustainable community layout.

thermal networks to capture the responses of building indoor temperatures given heating/cooling rates provided by the heating, ventilation and air-conditioning (HVAC) systems. Parameters in the models were estimated based on field measurements. The model details can be found in [8] and the obtained model for building j is formulated under a discrete-time state-space representation:

$$\begin{aligned} \mathbf{x}^j[i+1] &= \mathbf{A}^j\mathbf{x}^j[i] + \mathbf{B}_w^j\mathbf{w}^j[i] + \mathbf{B}_u^j Q_z^j[i] \\ y^j[i] &= \mathbf{C}^j\mathbf{x}^j[i] = x_z^j[i] \end{aligned}$$

where i indicates the time step, $\mathbf{w}$ is a vector of uncontrollable inputs or disturbances including weather conditions and internal heat gains, Q_z is the sensible cooling or heating provided to the space by the HVAC system and is the only controllable input. y or x_z is the zone air temperature.

B. Cooling Plant

In the case study, an air-cooled chiller is used as the central cooling plant providing constant temperature (8.5°C in the case study) chilled water to the different buildings. Chilled water flow rates in combination with the building supply fan speeds are modulated to meet the building cooling loads. In [9], a near-optimal control heuristic was developed for this chilled-water system that maintains minimum supply fan speeds and varies the chilled-water flow to meet individual building load. By virtue of the developed heuristic, the sensible cooling capacity for building j can be formulated as

$$Q_z^j = LR^j \cdot Cap_{rate}(\underline{T_{oa}})$$

where LR^j is the ratio of the cooling load in building j to the chiller total cooling capacity (Cap_{rate}). Only the sensible building loads are considered in this study because the simulation carried out in the case study involves dry weather conditions and a building moisture model is not considered here. Since the chiller leaving water temperature is constant, the chiller capacity is only a function of the outdoor temperature T_{oa}. Note that the heuristic helps remove the total airflow (m_a) from the design variables and make the following convex formulation possible. Define Pow_{ch} as the total power consumed by the chiller and chilled water pump. A 4$^{\text{th}}$ order convex polynomial fit was obtained that correlates Pow_{ch} to the total load ratio LR at each outdoor air temperature (see [9]):

$$Pow_{ch} = \text{Pow}_{\text{ch}}\left(LR, \underline{T_{oa}}\right) = \text{Pow}_{\text{ch}}\left(\sum\nolimits_{j=1}^{3} LR^j, \underline{T_{oa}}\right)$$

In addition to HVAC power consumption, other building electricity uses attributed to supply fan (supply fan power is constant providing the minimum airflow), lighting, computer and other electrical appliances, should also be accounted for in the optimal operation since demand is charged based on the total peak power. The non-HVAC power is assumed to be non-controllable and a typical diurnal profile for the non-HVAC power was obtained by averaging the actual measurements taken at Purdue CHPB for a whole month (see [9] for details). The same profile is applied to each day within the simulation test.

C. PV Generation

In this study, GridLAB-D ([10]), a power distribution system simulation tool, is used to provide PV power generation using the internal PV power model and based on TMY weather data for Indianapolis, IN. The case study uses a crystalline silicon PV panel with a face area of 33.4 m^2 and an efficiency of 0.2. For some time periods, generated solar power can be directly used to meet building electricity demands. Excess power can be stored in a battery that can be used at a later time. In this study, it is assumed that the excess PV power that cannot be used, or stored, cannot be sold back to the grid, so when the on-site battery is fully charged and there is no other electricity demand, the surplus PV power will be wasted.

D. On-Site Battery

A simple battery dynamic model is used ([11]):

$$SOC[i+1] = SOC[i] + P_c[i] - P_d[i] \quad (1)$$
$$0 \le SOC[i+1] \le SOC_{max} \quad (2)$$
$$0 \le P_c[i] \le P_{c,max} \quad (3)$$
$$0 \le P_d[i] \le P_{d,max} \quad (4)$$

where SOC is the battery state of charge, P_c and P_d are the charging and discharging rates, SOC_{max} is the battery capacity, $P_{c,max}$ and $P_{d,max}$ are the maximum charging and discharging rates for the battery. The case study uses a 4kWh battery (SOC_{max} = 4kWh) and assumes the battery can be drained from full capacity or fully charged from zero charge in 2 hours with maximum charging or discharging rates, i.e., $P_{c,max} = P_{d,max} =$ 2kW. Battery charging (η_c) and discharging (η_d) efficiencies are considered explicitly in the problem formulation in (7) and (8) and more details will be given in the following section.

III. Optimal Strategy

A 24-hr prediction horizon MPC problem is formulated to find the optimal control solution for the whole community. The goal is to optimize the building thermal control along with the energy flows among the various energy sources and users to minimize the operation cost within the look-ahead horizon. At each decision step, the MPC problem formulated in (5) to (18) is solved. In practice, weather and load conditions should be predicted in the beginning of each MPC step. This study assumes perfect prediction to illustrate the overall control approach. The cost function shown in (5) represents the total utility cost within the look-ahead horizon (Np steps) at a decision step k. k is reset to 1 at the beginning of a billing cycle. r_e, $r_{DC,l}$ and r_{gas} are the electricity energy rate ($/kWh), electricity demand charge rate ($/kW) and gas price ($/kWh), respectively. Time-of-use (TOU) energy rates are considered so the energy price is time indexed. The formulation can handle multiple demand charges associated with different rating periods denoted by P_l (the set of time indices in the l-th rating period), where $l = 1, ..., Nd$ and Nd is the number of demand rating periods. Q_{ht} is the gas heating rate and the gas price is assumed constant (0.03 $/kWh-heating in the case study). The first two terms in the cost function represent accumulated electricity energy cost and gas cost respectively, while the third term represents the incremental demand charge within the look-ahead horizon. $Pow_{thresh,l}[k]$ is the peak demand in the grid electricity purchase that occurs in rating period l within the previous $k-1$ time steps of the billing cycle. So the demand cost term is the incremental demand charge attributed to the additional peak demand beyond $Pow_{thresh,l}[k]$ that occurs within the look-ahead horizon. If the predicted peak demand is lower than $Pow_{thresh,l}[k]$, the demand cost term is 0. The billing cycle peak $Pow_{thresh,l}[k]$ needs to be updated after each MPC decision step if the current action leads to power consumption greater than the current $Pow_{thresh,l}[k]$, so $Pow_{thresh,l}[k+1] = \max(Pow_{thresh,l}[k], P_g[k])$ if $k \in P_l$ (P_g is the grid electricity purchase). $Pow_{thresh,l}[1]$ needs to be reset at the beginning of each billing cycle and [12] showed that a zero reset can provide near-optimal performance in most cases, i.e., $Pow_{thresh,l}[1] \leftarrow 0$ for each billing cycle.

$$\min \left\{ \begin{array}{l} \sum_{i=k}^{Np+k-1} \left\{ P_g[i] \cdot r_e[i] + \sum_{j=1}^{3} \left(Q_{ht}^j[i] \cdot r_{gas} \right) \right\} \\ + \sum_{l=1}^{Nd} \left\{ \max \left(\max_{i \in P_l} (P_g[i]) - \underline{Pow_{thresh,l}[k]}, 0 \right) \cdot r_{DC,l} \right\} \end{array} \right\} \tag{5}$$

$$\text{s.t.} \quad (j = 1, ..., N_{build} \text{ and } i = k, ..., k+Np-1)$$

$$Pow_{tot}[i] = \text{Pow}_{\text{ch}} \left(\sum_{j=1}^{3} LR^j[i], \underline{T_{oa}[i]} \right) + \underline{Pow_{nctrl}[i]} \tag{6}$$

$$P_g[i] = \max \left(Pow_{tot}[i] + P_c[i]/\eta_c - P_d[i] \cdot \eta_d - \underline{P_{PV,max}[i]}, 0 \right) \tag{7}$$

$$P_{PV}[i] = Pow_{tot}[i] + P_c[i]/\eta_c - P_d[i] \cdot \eta_d - P_g[i] \tag{8}$$

$$SOC[i+1] = SOC[i] + P_c[i] - P_d[i] \tag{9}$$

$$0 \leq SOC[i+1] \leq SOC_{max} \tag{10}$$

$$0 \leq P_c[i] \leq P_{c,max} \tag{11}$$

$$0 \leq P_d[i] \leq P_{d,max} \tag{12}$$

$$\mathbf{x}^j[i+1] = \mathbf{A}^j \mathbf{x}^j[i] + \mathbf{B}_w^j \underline{\mathbf{w}^j[i]} + \mathbf{B}_u^j Q_z^j[i] \tag{13}$$

$$Q_z^j[i] = -LR^j[i] \cdot \underline{Cap_{rate}(T_{oa}[i])} + Q_{ht}^j[i] + Pow_{fan} + m_{oa}^j[i] C_{pa} \left(\underline{T_{oa}[i]} - T_{RA} \right) \tag{14}$$

$$T_{z,lb}[i+1] \leq x_z^j[i+1] = \mathbf{C}^j \mathbf{x}^j[i+1] \leq T_{z,ub}[i+1] \tag{15}$$

$$m_{oa,min} \leq m_{oa}^j[i] \leq m_{oa,max} \tag{16}$$

$$0 \leq LR^j[i] \leq 1 \tag{17}$$

$$0 \leq Q_{ht}^j[i] \leq Q_{ht,max} \tag{18}$$

The optimization constraints are listed in (6) to (18). Pow_{tot} in (6) represents the sum of controllable and non-controllable power for all buildings. P_g in (7) represents the amount of electricity purchased from the power grid and P_{PV} in (8) is the actual electricity use from PV generation. Note that P_{PV} is not directly involved in the optimization but is an important intermediate variable for post-optimization analysis. $P_{PV,max}$ is the PV generation capacity calculated in Section II-C and the difference between $P_{PV,max}$ and P_{PV} represents the amount of PV power that is wasted.

Remark 1: An alternative and more intuitive formulation for (7) and (8) is

$$P_g[i] = Pow_{tot}[i] + P_c[i]/\eta_c - P_d[i] \cdot \eta_d - P_{PV}[i] \tag{19}$$

$$0 \leq P_{PV}[i] \leq \underline{P_{PV,max}[i]} \tag{20}$$

but the first inequality in (20) would compromise convexity in the overall formulation (Pow_{tot} is strictly convex and its hypograph is not convex). The formulation in (7) and (8), however, can preserve convexity and is equivalent to (19) and (20) except that (7) and (8) ensure the maximum utilization of PV power whenever possible, which should be expected in the optimal solution.

Constraints in (9) to (12) come from the battery model developed in Section II-D.

Remark 2: An important constraint in the battery operation is to prevent simultaneous charging and discharging. It is difficult to formulate this constraint in a convex form. For example, $P_c \cdot P_d = 0$ and $\min(P_c, P_d) \leq 0$ are two possible formulations but both are non-convex. However, the efficiency losses associated with the battery charging and discharging processes that are explicitly considered in (7) and (8) will intrinsically prevent simultaneous charging and discharging in the optimal solution. This will eliminate the need of an explicit constraint which helps to preserve convexity.

The set of constraints shown in (13) come from the building dynamic models developed in Section II-A. Constraints in (14) calculate the net sensible cooling/heating rates by considering different energy sources: from cooling coil, gas heating, constant fan heat (Pow_{fan}) and ventilation. Note that this constraint is originally bilinear since the return air temperature T_{RA} is the design variable x_z^j. However, this is simplified to a linear constraint by fixing the return air temperature to a constant nominal value (see [9] for details). m_{oa} is the outdoor airflow rate which should be above the ventilation requirement $m_{oa,min}$ and below the fixed total airflow $m_{oa,max} = m_a$ for each building, which is reflected in constraints (16). Constraints (15) are used to ensure indoor thermal comfort. The upper and lower bounds, $T_{z,lb}$ and $T_{z,ub}$, can vary depending on the occupancy status of the building. Constraint in (17) comes from the requirement that the sum of cooling rates provided to different buildings needs to be smaller than the chiller's cooling capacity. Heating capacity constraints are shown in (18).

The formulated MPC problem is convex, and is solved with the convex programming package CVX in Matlab ([13]) with the SDPT3 solver ([14]).

IV. Baseline Strategy

A baseline control strategy was also simulated to assess the cost savings potential with the optimal control solution. The baseline control implements a night setup cooling setpoint trajectory and a night setback heating trajectory for the building indoor temperatures. Minimum cooling or heating is enabled to maintain the indoor temperatures within the temperature band. Algorithm 1 shows a baseline algorithm for the battery and PV operation. This algorithm only uses battery to collect excess PV generation when building electrical demands are low. During the high building-load periods, electricity stored in the battery is used first to meet the building demands and electricity purchase from the grid is only allowed when the battery is fully drained.

Algorithm 1 : *Baseline strategy*

```
Initialize SOC[1] = 0
for i = 1 to Nsim do
  if Pow_tot[i] − P_PV,max[i] < 0 then
    P_g[i] ← 0
    SOC[i + 1] = min(SOC[i] + (P_PV,max[i] − Pow_tot[i]) · η_c, SOC_max)
    P_c[i] ← SOC[i + 1] − SOC[i]
    P_d[i] ← 0
  else if Pow_tot[i] − P_PV,max[i] ≥ 0 and Pow_tot[i] − P_PV,max[i] < SOC[i] · η_d then
    P_g[i] ← 0
    SOC[i + 1] ← SOC[i] + (P_PV,max[i] − Pow_tot[i])/η_d
    P_c[i] ← 0
    P_d[i] ← (Pow_tot[i] − P_PV,max[i]) /η_d
  else if Pow_tot[i] − P_PV,max[i] ≥ SOC[i] · η_d then
    P_g[i] ← Pow_tot[i] − P_PV,max[i] − SOC[i] · η_d
    SOC[i + 1] ← 0
    P_c[i] ← 0
    P_d[i] ← SOC[i]
  end if
  P_PV[i] = Pow_tot[i] + P_c[i]/η_c − P_d[i] · η_d − P_g[i]
end for
```

V. Case Study Results

The case study utilizes typical summer TOU electricity tariffs shown in Table I. Electricity energy cost differs slightly between on-peak, mid-peak and off-peak periods and only an anytime peak demand charge is present. So there is only one demand rating period and $Nd = 1$ in the cost function in (5). The solution is implemented in a MPC scheme with a 24-hr look-ahead horizon ($Np = 24$) and an 1-hr decision step (the same as the building dynamic model time step). Zone temperature lower and upper bounds assume $T_{z,lb} = 20.5°C$ and $T_{z,ub} = 24.5°C$ during unoccupied periods and $T_{z,lb} = 21.5°C$ and $T_{z,ub} = 23.5°C$ during occupied periods. The occupied period starts from 9am and ends at 9pm every day and the rest of the time is unoccupied. The minimum outdoor air intake is $m_{oa,min} = 250$ CFM (0.14 kg/s) for ventilation and the maximum is $m_{oa,max} = 1200$ CFM (0.67 kg/s) which is the fixed total airflow for all buildings. Actual weather measurements from June 2015 were used as external excitations in the simulation test and perfect weather prediction was assumed in the MPC optimization.

The whole month simulation results associated with the baseline and optimal control strategies are shown in Fig. 2 and Fig. 3, respectively. The top subplot shows the variations of building indoor temperatures. The middle subplot shows variations of the non-HVAC power for all three buildings and also the total chiller power. The bottom subplot shows the energy intakes from the different sources: P_g-electricity purchase from the grid; P_d-battery discharge; PV-actual electricity use from PV generation (P_{PV} in (8)). The trajectory of the peak demand in the electricity purchase from the grid ($Pow_{thresh,l}$ in (5)) is also shown in the bottom plot denoted by $Peak$. Negative values in the bottom subplot represent energy charged into the battery which can be from either grid purchase or PV generation.

With the baseline strategy, the right amount of cooling

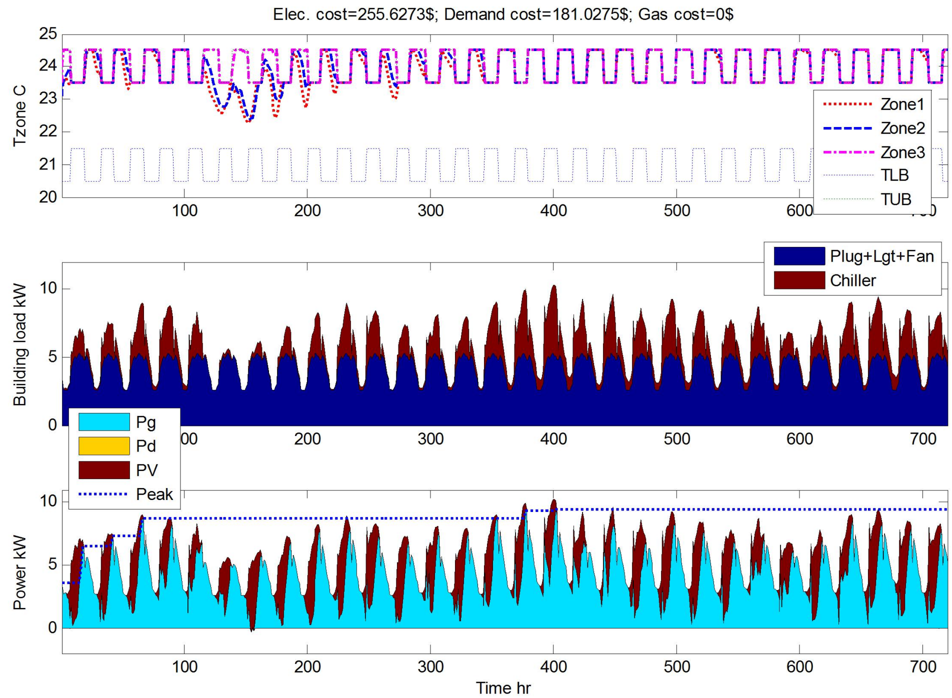

Fig. 2. Baseline control results.

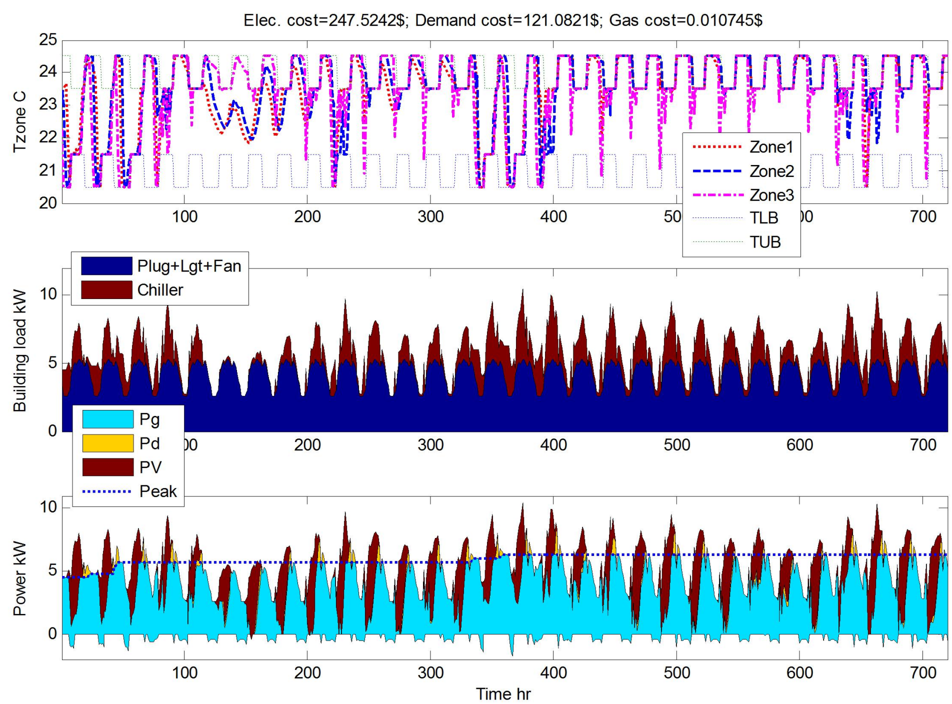

Fig. 3. Optimal control results without economizer operation.

is provided to prevent the indoor temperatures from rising beyond the temperature upper bounds. The total building electricity demand has a peak occurring at hour 400. The baseline strategy only allows the battery to collect excess PV power. The battery is charged and discharged only once within the whole simulation month which occurs at hour 160. That is because each office (case study building) houses dozens of continuously operating computers leading to significant building power demand during unoccupied periods which consumes all PV power generation for most of the time. It is expected that in typical commercial buildings, the battery will be used more often.

Fig. 3 shows the optimal control results without economizer operation (outdoor air flow is maintained at the minimum level throughout the whole simulation period by setting $m_{oa,max} = m_{oa,min}$). It can be seen that the optimal control solution performs load shifting to reduce the on-peak energy use and also to reduce the total peak demand

TABLE I
SUMMER TOU TARIFFS WITH DEMAND CHARGES

Rate periods	**Electricity price ($/kWh)**	**Hours**	**Demand charge**
On-peak	0.108	Noon-6PM	19.2 $/kW anytime peak demand
Mid-peak	0.089	8AM-Noon; 6PM-11PM	
Off-peak	0.064	Other hours	

TABLE II
COMPARISON OF ELECTRICITY COSTS FOR THE VARIOUS STRATEGIES

Scenario	**Energy cost ($)**	**Demand cost ($)**	**Total cost ($)**
Baseline w/o PV, battery	372 (45.6% ↗)	197 (8.8% ↗)	569 (30% ↗)
Baseline	255.6	181	436.6
Optimal	247.5 (3.2% ↘)	121.1 (33.2% ↘)	368.6 (15.6% ↘)
Optimal w/ econ.	231.6 (9.4% ↘)	116.5 (35.6% ↘)	348.1 (20.3% ↘)

leading to lower operation cost. Two types of load shifting can be observed: 1) during the on-peak days such as hours 340 to 400 and also in the first few days of the month, all buildings are precooled in evening and early morning to shift the on-peak cooling energy use to off- or mid-peak hours; 2) electricity is purchased from the grid to fully charge the battery within off-peak hours and the battery is fully drained during the on-peak periods to reduce the on-peak electricity purchase for almost all simulation days. In addition, different buildings carry out precooling at different times of the day to maintain a flat total power profile. With optimal scheduling of the building thermal loads and battery operation, the peak demand in the electricity purchase is significantly reduced, and a demand cost savings of 30%, an energy cost savings of 3.2% and a total cost savings of 15.6% can be achieved as shown in Table II. With optimal economizer operation, much higher energy cost savings can be achieved and the total cost savings is increased to 20.3%. To understand the economic benefit of the on-site PV and battery system, a baseline control case without PV generation and batteries was also simulated with the night setup/setback control strategy. It can be seen that total electricity cost for this case is 30% higher than the baseline control case with an on-site PV and battery system.

VI. CONCLUSION

This paper presented a convex-optimization-based control strategy for a sustainable community with multiple buildings and with on-site PV electricity generation and batteries. A MPC problem was formulated to obtain the optimal schedules of the energy flows among the different sources and electricity end users. With certain manipulation in the formulation, the MPC problem was expressed as a convex optimization problem and was then solved with a convex solver package. To benchmark the performance of the proposed control solution, a baseline operation strategy was also simulated with a conventional night setup/setback indoor temperature control and a heuristic strategy for charging and discharging the on-site battery. A 35% demand cost savings and a 20% total cost savings were demonstrated using a three-building case study with a 33.4 m^2 PV panel and a 4kWh battery. The optimal operation strategy proposed in this paper can also be used to properly size the PV panel and battery for a sustainable community.

For optimal energy management of sustainable communities or cities with certain complexities, a distributed control strategy such as multi-agent control is more suitable since the distributed approach is scalable and can better handle complex optimization problems and also because of the distributed nature of the energy sources/users in a community or city. For distributed control approaches, convexity is critical to guarantee convergence in the distributed and cooperative optimization algorithms. Future studies will build on top of the work presented in this paper and develop a multi-agent controller for optimal community- or city-level energy management.

REFERENCES

[1] Y. Zong, L. Mihet-Popa, D. Kullmann, A. Thavlov, O. Gehrke, and H. W. Bindner, "Model predictive controller for active demand side management with pv self-consumption in an intelligent building," *IEEE PES Innovative Smart Grid Technologies Europe*, 2012

[2] J. Pascual, J. Barricarte, P. Sanchis, and L. Marroyo, "Energy management strategy for a renewable-based residential microgrid with generation and demand forecasting," *Applied Energy*, 2015

[3] B. W. Jones and R. Powell, "Evaluation of distributed building thermal energy storage in conjunction with wind and solar electric power generation," *Renewable Energy*, 2015

[4] Ikeda, Shintaro, and Ryozo Ooka. "Metaheuristic optimization methods for a comprehensive operating schedule of battery, thermal energy storage, and heat source in a building energy system." *Applied Energy*,2015

[5] Y. Lu, S. Wang, Y. Sun, and C. Yan, "Optimal scheduling of buildings with energy generation and thermal energy storage under dynamic electricity pricing using mixed-integer nonlinear programming", *Applied Energy*, 2015

[6] G. Mokhtari, G. Nourbakhsh, and A. Gosh, "Optimal Sizing of Combined PV-Energy Storage for a Grid-connected Residential Building", *Advances in Energy Engineering*, 2013

[7] X. Li, J. Wen, and A. Malkawi, "An operation optimization and decision framework for a building cluster with distributed energy systems," *Applied Energy*, 2016

[8] Cai, Jie. A low cost multi-agent control approach for building energy system management. Ph.D. Dissertation, Purdue University, 2015.

[9] Cai, Jie, James E. Braun, Donghun Kim, and Jianghai Hu. "A multi-agent control based demand response strategy for multi-zone buildings." *American Control Conference (ACC)*, 2016.

[10] D. P. Chassin, K. Schneider, and C. Gerkensmeyer, "GridLAB-D: An open-source power systems modeling and simulation environment," *IEEE/PES Transmission and Distribution Conference and Exposition*, 2008.

[11] Morais, H., Kadar, P., Faria, P., Vale, Z. A., & Khodr, H. M. "Optimal scheduling of a renewable micro-grid in an isolated load area using mixed-integer linear programming." *Renewable Energy*, 2010.

[12] Cai, Jie, James E. Braun, Donghun Kim, and Jianghai Hu. "General approaches for determining the savings potential of optimal control for cooling in commercial buildings having both energy and demand charges." *Science and Technology for the Built Environment*, 2016.

[13] Grant, Michael, Stephen Boyd, and Yinyu Ye. CVX: Matlab software for disciplined convex programming, 2008.

[14] Toh, K.C., Todd, M.J. and Tutuncu, R.H., "SDPT3 a Matlab Software Package for Semidefinite Programming". *Optimization Methods and Software*, 1999.